CHARACTERIZING THE MODIFICATION SEQUENCE OF SIMPLE IMPACT CRATERS IN MULTIPLE SETTINGS ON MARS. C. B. Hundal[1], W. A. Watters[1], C. I. Fassett[2], J. Maciuch[1]. [1]Dept. Astronomy, Whitin Observatory, Wellesley College, Wellesley, MA 02481 (chundal@wellesley.edu). [2]NASA Marshall Space Flight Center, Huntsville, AL 35805.

Introduction: Studying the morphology of craters on other worlds has been the primary means of learning more about crater formation and the conditions and processes that modify them. A number of previous studies have characterized the modification sequence of craters on the Moon, finding that linear diffusion models provide a useful description of the evolution of lunar crater morphology [1,2]. Comparable studies for martian craters have been challenged by Mars' more complex weathering and erosion processes [3,4,5]. The use of Digital Elevation Models (DEMs) created from High Resolution Imaging Science Experiment (HiRISE; 25 cm/px), rover data, and Context Camera (CTX; 6 m/px) imagery has permitted the study of the morphometry of small impact craters and their long-term evolution [e.g., 5-9].

A major goal of recent work has been to identify which variations in shape are due to (a) the nature of the impact itself (e.g. properties of target material, impact speed, impact angle, etc.) versus (b) the local conditions and processes which modified the crater's shape over time. The variation of the initial shape of craters has been largely characterized by previous studies [e.g. 9,10,11]. The present work contributes to an ongoing investigation of the modification sequence of small craters and how this depends on terrain properties [12,13].

Crater database: We have assembled a database of 7418 simple primary craters with diameters between 500 m and the simple/complex transition (5-8 km on Mars). Craters were selected from CTX images which had stereo pairs in Amazonis Planitia, Terra Sabaea, and Sinai Planum. These regions were chosen to represent (a) young, relatively strong targets, (b) older, regolith-dominated terrains, and (c) an intermediate case, respectively. Here, we report morphometric measurements for craters having $D > 1$ km. This subset contains 506 total craters: 282 in Amazonis, 90 in Terra Sabaea, and eight in Sinai Planum.

Qualitative attributes were assigned to each crater by visual inspection to identify additional factors relating to initial shape and modification. Several attributes, such as distinctive hallmarks of flooding by volcanic flows, significant modification by ice-related processes, and association with clusters of probable secondaries, were used to identify and remove craters whose shapes were not dominantly determined by dry, long-acting surface processes that have modified primary craters (e.g. wind, thermomechanical weathering, soil creep, and mass wasting).

DEMs: CTX stereo pairs were identified in accordance with the parameter limits described in [14], and were generated for image pairs containing the craters in our study using the Ames Stereo Pipeline [15]. DEMs were then post-processed according to the procedure outlined in [9].

Parameter measurements: We measure "length scales of steepening" ("steepening lengths," for short), defined as the distances over which transitions in slope and curvature occur along radial topographic profiles of the upper and lower crater cavity. An automated process was used to determine the radial distance between points of interest (POIs) along elevation profiles extending from the center to $1.25R$, where R is the manually-estimated radius. These points include the point of Most Negative Curvature (MNC, identical to the topographic rim in well-preserved craters), and positions where fractions of the maximum wall slope are first reached while moving centerward or outward.

The position of the inflection point (the point of maximum slope, s_{max}, along a radial profile) is often difficult to determine accurately because the slope is highly uniform in this region. We therefore measure "steepening lengths" instead from positions corresponding to specific fractions of maximum slope, where the slope is changing more rapidly as a function of radial position. Like the inflection point, the position of the rim is difficult to pinpoint in highly degraded craters, whose cavity and surroundings are not separated by a topographic high because their rims have been destroyed. For this reason, we use the radial position of most negative curvature instead (R_{MNC}).

Each "steepening length" was measured in 12 non-overlapping radial profiles and averaged; the uncertainty of this mean was estimated from the variation between profiles in a single crater.

Results: Figure 1 shows crater rim-to-floor depth (d) versus visually-estimated diameter (D) for the three study areas, highlighting the relatively deep and young Amazonis craters. Figures 2 and 3 are box plots that show a "steepening length" for the lower and upper cavity (λ_L and λ_U, respectively) plotted versus decreasing depth/diameter (i.e., this axis represents increasing modification and time toward the right). The value of λ_L was measured between the position of $0.25s_{max}$ on the lower cavity wall and R_{MNC}. The value of λ_U was

measured between the position of $0.5s_{max}$ on the upper cavity wall and R_{MNC}.

Figure 2 shows a clear decrease in λ_L/R as craters become shallower. That is, the cavity wall steepens more abruptly (while moving outward) over time, implying wider floors. This is consistent with sediment infilling derived from nonlocal sources. By contrast, the value of λ_U/R exhibits no discernible dependence on d/D, in marked contrast to the evolution of lunar craters [13]. This suggests, as our previous work has done [12], that the modification of martian crater shape is dominantly driven by aeolian sediment infilling, and that diameter-scaled depth is hence largely decoupled from the evolution of the shape of the upper cavity.

We also find that the degree of crater-wide variation in some "steepening lengths" and in R_{MNC} increases along with d/D. We suggest this is possibly on account of asymmetries in sediment distribution in crater floors, although may be the consequence of uneven erosion of crater rims as well.

Future work: To the extent that the upper cavity shape preserves a record of modification and processes driving erosion on Mars, it may be fruitful to compare the dependence of upper cavity shape parameters to diameter-normalized rim height or the maximum crater wall slopes. A second short-term objective is to increase the size of our database in order to examine terrain-dependent effects.

Acknowledgments: Work supported by NASA Mars Data Analysis program grant (NNX15AM40G).

References: [1] Soderblom, L.A., & Lebofsky, L.A., (1972) *JGR*, 77, *279–296;* [2] Fassett, C.I., & B.J. Thomson (2014) *JGR Planets*, *119*, *2255-2271;* [3] Craddock, R. A., et al. (1997) *JGR Planets*, 102, pp. 13321–13340*;* [4] Forsberg-Taylor, N.K. (2004) *JGR-Planets*, 109, E05002; [5] Golombek et al. (2014) *JGR-Planets*, 119, pp. 2522–2547; [6] McEwen, A. et al., *Icarus* 176, pp. 351-381, 2005; [7] McEwen, A. et al., (2007) *JGR-Planets*, 112, E05S02; [8] Calef, F.J. et al. (2009) *JGR-Planets*, 114 (E13), E10007; [9] Watters et al. (2015) *JGR-Planets*, 120, pp. 226–254; [10] Stopar et al. (2017) *Icarus*, 298, pp. 34-48; [11] Daubar et al. (2014) *JGR-Planets*, 119, pp. 2620-2639; [12] Watters, W.A. et al. (2016) *LPSC 47*, #2972; [13] Watters, W.A. and C. Fassett (2016) *Fall AGU*, #EP53C-0955; [14] Becker, K.J. et al. (2015) *LPSC 46*, #2703; [15] Moratto, Z., et al., (2010) *LPSC 41*, #2364;

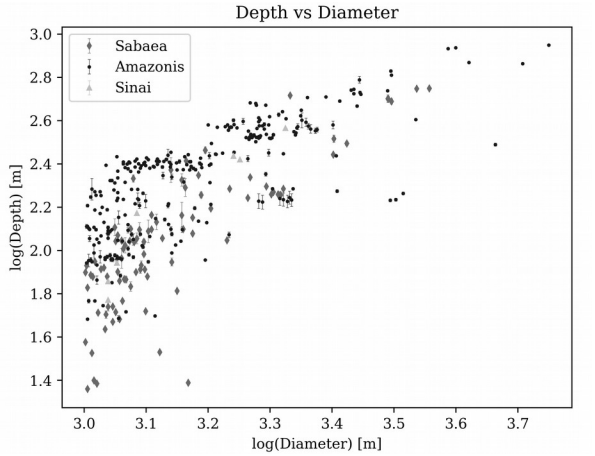

Figure 1: Rim-to-floor depth vs. rim-to-rim diameter for the N = 506 craters in our database with D > 1 km.

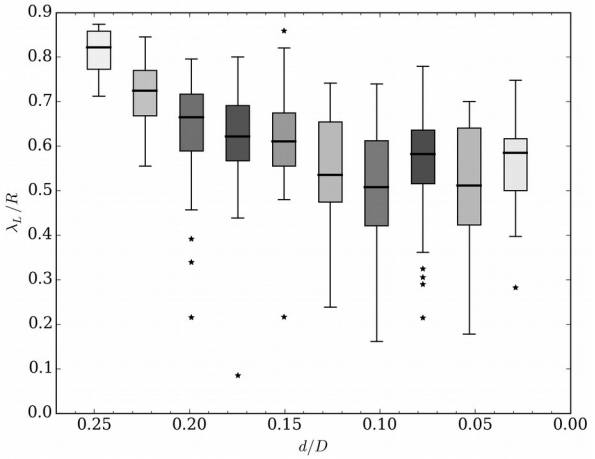

Figure 2: Radius-normalized steepening length for lower cavity vs. d/D. Crater floors widen and flatten as depth decreases over time. Box shade is proportional to number of craters represented. (N = 506)

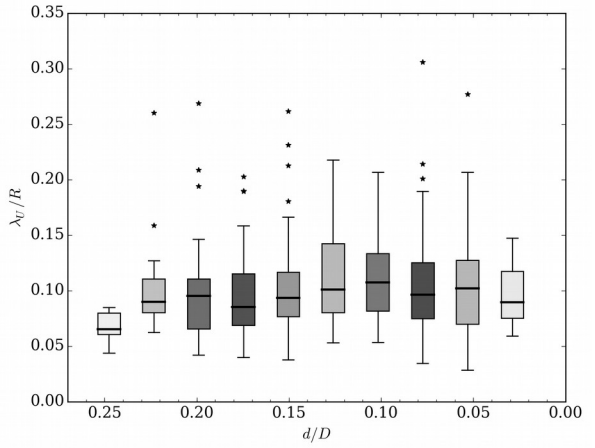

Figure 3: Radius-normalized steepening length for upper cavity vs. d/D. The shape of the upper crater wall and rim is largely independent of diameter-normalized crater depth.